

Electronic Supplementary Information for “Bio-inspired three-dimensional self-patterning of functional coatings for PDMS microfluidics”

Tianzhun Wu,^{*ab} Hiroaki Suzuki,^{bc} Yuquan Su^a, Zikang Tang^a, Liang Zhang^d and Tetsuya Yomo^{*bce}

^a School of Physics and Engineering, Sun Yat-sen University, Xingang West 135, Guangzhou 510275, PR China. E-mail: wutzh@mail.sysu.edu.cn.

^b Exploratory Research for Advanced Technology (ERATO), Japan Science and Technology Agency (JST), 1-5 Yamadaoka, Suita, Osaka 565-0871, Japan

^c Graduate School of Information Science and Technology, Osaka University, 1-5 Yamadaoka, Suita, Osaka 565-0871, Japan

^d Key Lab for New Drugs Research of Traditional Chinese Medicines Shenzhen, Research Institute of Tsinghua University in Shenzhen, Shenzhen High-Tech Industrial Estate, Shenzhen 518057, PR China.

^e Graduate School of Frontier Biosciences, Osaka University, 1-5 Yamadaoka, Suita, Osaka 565-0871, Japan. E-mail: yomo@ist.osaka-u.ac.jp.

M1: A movie showed the evaporation process of ethanol on as-treated PDMS microchannels.

CYTOP Concentration	CA on smooth PDMS /°	CA on rough PDMS /°
1:2	110.3	113.6
1:5	105.6	111.5
1:10	101.1	108.4

Table S1. Contact angles (CAs) of diluted CYTOP droplets on smooth and rough PDMS transferred from SU-8 after 3 min O₂ plasma etching

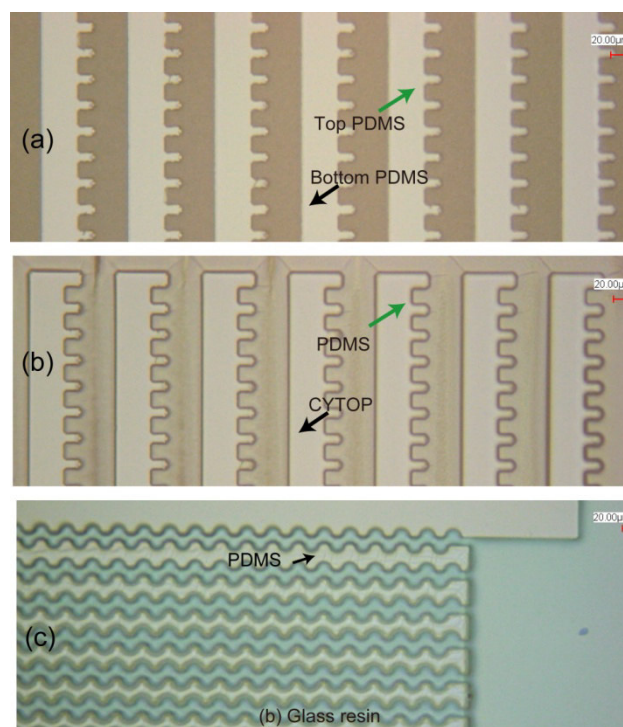


Fig. S2 Microscopic pictures showing CYTOP and glass resin coatings on rough PDMS channels. (a) Before Coating. (b) 1:5 diluted CYTOP coating. (c) Glass resin coating (GR-650F, Techneglas Co.). Blue dye was added for clear visualization.

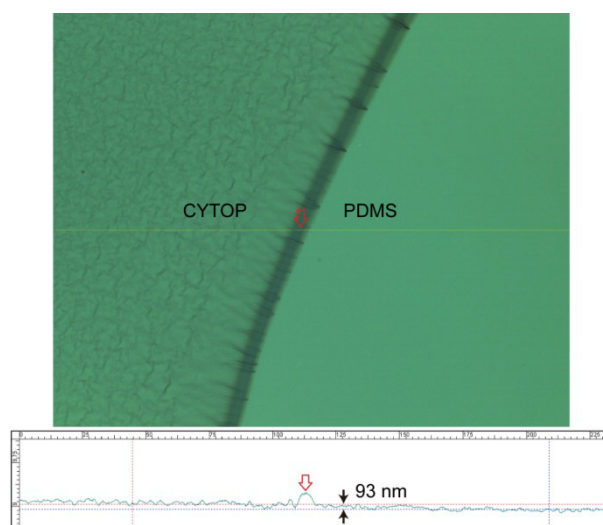


Fig. S3 The coffee ring effect (thicker edge where the arrow is placed) for 1:5 diluted CYTOP coating on the smooth PDMS after curing. The surface profile was measured by the confocal microscope Axio CSM 700.

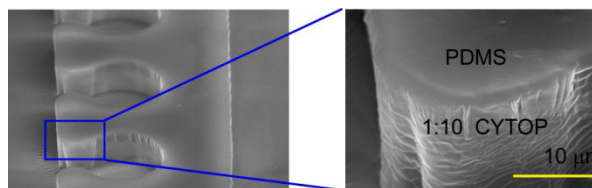


Fig. S4. Wrinkles of thin CYTOP coating on PDMS after curing.

S5: Estimation of evacuation time of liquid from a unit

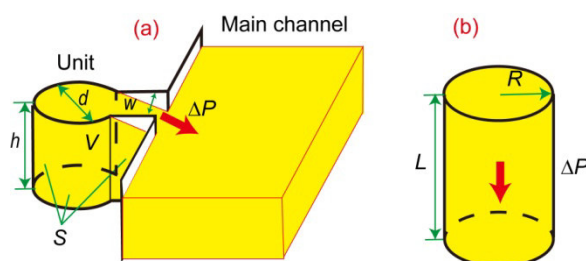


Fig. S5 Illustration of liquid flow in a unit (a) during evaporation and its simplified case (b).

Clogging is regarded to depend on the evacuation time of liquid from a unit (microchannel or microchamber) to the main fluidic channel during evaporation, as illustrated in Fig. S5a, where the driving pressure ΔP is due to the smaller exposed area of the unit than that of the main channel leads to slower evaporation. Possibility of clogging increases with longer evacuation time, since the viscosity increases and the liquid flow becomes slower during the constant evaporation process. We assume a simplified case of laminar flow that viscous drag is dominant during this process (Fig. S5b), and gravity is ignored. It is not strict but simple enough to model the friction of an open-channel flow as the viscous drag in a cylindrical pipe with the following equivalents

$$\begin{cases} \pi R^2 L = V \\ 2\pi R L = S \\ Q_v = \frac{\pi R^4}{8\eta L} \Delta P \Rightarrow t = \frac{\eta}{2\pi^2 \Delta P} \left(\frac{S^3}{V^2} \right)^2 \\ t = \frac{V}{Q_v} \end{cases}$$

where R , L , S , V are respectively the hydraulic radius, pipe length, wet surface area (including the bottom area and the sidewall area of a unit) and volume of a unit. η is the average dynamic viscosity of the liquid flow during evaporation, which are simply assumed to be same for all tested samples. As the conclusion, the evacuation time as well as the clogging possibility is related to S^3/V^2 which is a dimensionless parameter.

The values of S , V were obtained by using the ImageJ software, and CYTOP 1:10 diluted was used as the solution. The data used for Fig. 4 is listed as following (h, d, w are illustrated in Fig. S5):












No.	Unit shape	Symbol	$h/\mu\text{m}$	$d/\mu\text{m}$	$w/\mu\text{m}$	S^3/V^2	Clogging ratio
1	Two openings		9.8	21.4	12.6	28.36	0
2	Rectangle		42.8	15.6	21.5	79.01	0
3	Rectangle		13.2	42.2	22.2	81.3	0
4	Two circles		18.4	20.0	12.7	57.35	0
5	Two circles		8.5	10.0	5.2	93.92	0
6	Two circles		18.4	10.2	5.9	140.32	0.26
7	Circle		9.4	18.2	12.0	74.16	0
8	Circle		9.4	18.1	10.7	81.93	0.42
9	Circle		9.4	16.4	8.4	88.28	0.95
10	Circle		13.2	18.3	6.1	89.4	0.83
11	Circle		13.2	19.2	5.7	90.6	0.90

Table S5. Experimental data used for Fig.4.

S6: Calculation of the pressure drop of a microchannel

The pressure drop ΔP of a channel with rectangle cross-section can be simplified as¹

$$\Delta P = \frac{C(\alpha)}{32} \frac{\mu L Q P^2}{A^3} \Rightarrow \Delta P \propto \frac{(1+h/w)^2}{wh^3},$$

where $C(\alpha)$ is a constant related with the aspect ratio α , defined as either height/width or width/height so $0 \leq \alpha \leq 1$. μ is the dynamic viscosity of the fluid, and Q is the volumetric flow rate. Here, w is the channel width, L is the channel length and $P=2(w+h)$ and $A=wh$ are the perimeter and area, respectively, of a cross section of the channel. In our design, $h=42 \mu\text{m}$, the narrowest channel width $w=50 \mu\text{m}$, which contributes to most of ΔP compared with wide main channel ($w>1 \text{ mm}$), so that $\alpha=h/w=0.84$, according to Ref. 1, $C(\alpha)=57.3$. $L \approx 2.2 \cdot 10^{-3} \text{ m}$, $P = 1.84 \cdot 10^{-4} \text{ m}$, $A=2.1 \cdot 10^{-9} \text{ m}^2$. For the input of silicone oil, $Q=1200 \mu\text{L}/h=3.3 \cdot 10^{-9} \text{ m}^3/\text{s}$, $\mu=1 \cdot 10^{-2} \text{ Pa}\cdot\text{s}$, so that $\Delta P \approx 475 \text{ KPa}$, close to the reported bonding strength of PDMS-glass after O_2 plasma activation.²

References

- 1 W.-H. Tan and S. Takeuchi, *Proc. Natl. Acad. Sci. USA*, 2007, **104**, 1146–1151.
- 2 J. Kim, R. Surapaneni, and B. K. Gale, *Lab Chip*, 2009, **9**, 1290.